Nonlinear inelastic scattering of electrons at an optical standing wave

M. Kozák*

Faculty of Mathematics and Physics, Charles University, Ke Karlovu 3, 12116 Prague 2, Czech Republic

(Received 21 February 2018; published 11 July 2018)

We investigate higher-order nonlinear inelastic scattering of electrons at an optical standing wave formed by two light waves with the same frequencies in vacuum. Initial conditions necessary for efficient scattering are obtained from the semiclassical energy and momentum conservation laws for all nonlinear orders. The stationary scattering potential in the electrons' rest frame is derived from the perturbative solution of the classical relativistic equation of motion for the four-photon scattering process. The amplitude of the electron velocity modulation introduced during higher-order scattering processes is calculated numerically. The proposed inelastic interaction leads to a periodic modulation of the electrons' energy and longitudinal momentum at a higher harmonic frequency of the driving light waves.

DOI: 10.1103/PhysRevA.98.013407

I. INTRODUCTION

Scattering of matter waves at a free-space optical grating formed by the periodic intensity distribution of an optical standing wave is known as the Kapitza-Dirac effect [1]. The interaction is driven by the ponderomotive potential arising from the electron quiver motion in the nonuniform electromagnetic field of the two counterpropagating light waves with field amplitudes $\boldsymbol{E_0}\cos(\omega t - kx)$ and $\boldsymbol{E_0}\cos(\omega t + kx)$. Depending on the experimental conditions, the process takes place either in the quantum coherent regime, in which coherent diffraction peaks are observed in the particle transverse momentum [2–4], or in the classical scattering regime [5–7]. The latter leads to generation of two broad rainbow peaks in the particle transverse momentum distribution [6,7].

The physics of an individual scattering event can be described in two equivalent ways. In the particle picture, one photon with energy $\hbar\omega$ and momentum $+\hbar\mathbf{k}$ is absorbed by the particle while another photon with energy $\hbar\omega$ and momentum $-\hbar\mathbf{k}$ is emitted. The process is energy conserving and the particle momentum changes by two photon recoils. In the diffraction picture, the matter wave with de Broglie wavelength of $\lambda_{\mathrm{dB}} = h/p$ coherently diffracts at the periodic ponderomotive potential $U_{\mathbf{p}} = (kq^2E_0^2)/(m_0\omega^2)\cos(2kx)$, where q and m_0 are the electric charge and mass of the particle, respectively.

The Kapitza-Dirac effect with atoms and electrons has been studied both theoretically [8–10] and experimentally [2–6,11]. The coherent electron diffraction peaks were observed in the Raman-Nath regime corresponding to diffraction at a thin grating [3] and the Bragg regime corresponding to the thick grating case [4]. The relativistic [12–15] and spin effects [16–19] have been theoretically studied. Further, inelastic ponderomotive scattering of electrons at an optical traveling wave was proposed [20,21] and experimentally demonstrated [22,23]. Due to the time-correlated energy modulation imprinted to the electrons accelerated to ∼keV energies, this process allows the generation of attosecond electron pulse trains [23] while being driven by two optical waves at different frequencies.

An alternative technique allowing energy and momentum transfer between electron wave packets and light relies on the inelastic scattering of electrons at optical near fields of nano-objects with subwavelength dimensions or the field discontinuity at thin membranes. Using this approach, both the quantum [24–29] and the classical [30,31] inelastic scattering regimes have been demonstrated. The subcycle electron energy modulation was directly observed [32–35] and applied to compression of electron beams for ultrafast diffraction experiments [34,35].

In this paper we propose a different type of inelastic interaction leading to a time-dependent energy modulation of subrelativistic electrons. The interaction is based on higher-order nonlinear components of the electron quiver motion in electromagnetic fields of a high-intensity optical standing wave beyond the dipole approximation. A similar effect was already theoretically considered for elastic electron scattering at two counterpropagating light waves at different frequencies [36]. For the energy conserving processes with $N\omega_1 = L\omega_2$ (ω_1 and ω_2 are frequencies of the two counterpropagating light waves; N, L are positive integer numbers), there exists a periodic stationary potential, which is either velocity dependent (odd number of photons involved in the scattering, $\omega_1 = 2\omega_2$) or velocity independent (even number of photons, $\omega_1 = 3\omega_2$) [36]. The diffraction of the electrons occurs for angles of incidence θ fulfilling the Bragg condition $2d\sin\theta = \lambda_{\mathbf{dB}}$, where d is the spatial period of the stationary potential. The same condition is obtained from the energy and momentum conservation laws for the process, in which the electron absorbs N photons from one wave and emits L photons to the second wave. Due to the opposite directions of momenta $\mathbf{k_1}$ and $\mathbf{k_2}$ of the two driving light fields, the electron transverse momentum changes by $N\mathbf{k_1} - L\mathbf{k_2}$.

II. THEORY

In our proposed scheme, the electrons propagating along the x axis with velocity $\mathbf{v_i} = (v_x,0,0)$ inelastically scatter at an

*kozak@karlov.mff.cuni.cz

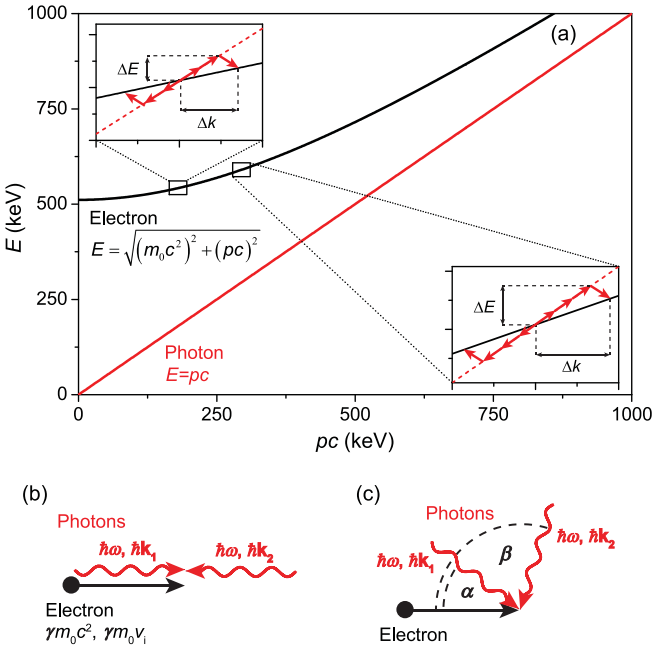

FIG. 1. (a) Dispersion relations of an electron (black curve) and a photon (red curve) in vacuum. The insets show three-photon (upper inset) and four-photon (lower inset) scattering processes, which conserve both momentum and energy. (b) Experimental geometry of the proposed nonlinear scattering, in which the electron copropagates with one of the two counterpropagating light waves with wave vectors $\boldsymbol{k_1} = (k,0,0) = -\boldsymbol{k_2}$ and frequency ω. (c) Generalized geometry, where the two light waves are incident under the angles α and β with respect to the electron propagation direction.

optical standing wave formed by two counterpropagating optical waves with wave vectors $\boldsymbol{k_1} = (k,0,0) = -\boldsymbol{k_2}$ oscillating at the same frequency ω [Fig. 1(b)]. The semiclassical relativistic energy and momentum conservation laws are fulfilled for higher-order scattering processes involving absorption and emission of more than two photons [see the photon and electron dispersion relations in Fig. 1(a)]. Because the momenta of all interacting particles are parallel, only the longitudinal electron momentum component p_x changes. For the case where N photons are absorbed and L photons are emitted we can write

$$\Delta E = (\gamma_\mathbf{f} - \gamma_\mathbf{i}) m_0 c^2 = (N-L)\hbar\omega, \tag{1}$$

$$\Delta p_x = \gamma_\mathbf{f} m_0 v_\mathbf{f} - \gamma_\mathbf{i} m_0 v_\mathbf{i} = (N+L)\frac{\hbar\omega}{c}. \tag{2}$$

Here ΔE is the change of the electron energy, Δp_x is the change of the longitudinal electron momentum, c is the speed of light, and $\gamma_{\mathrm{f,i}} = (1 - v_{\mathrm{f,i}}^2/c^2)^{-1/2}$ are the relativistic Lorentz factors corresponding to the final and initial electron velocities v_f and v_i. Equations (1) and (2) are solved to obtain the initial electron velocity v_i. When the condition $\hbar\omega/(m_0c^2) \ll (\gamma_\mathbf{i}^2 - 1)$ is met (with a common photon energy $\hbar\omega = 1.5\,\mathrm{eV}$, this condition gives $v_\mathrm{i} \gg 1.7\times10^{-3}c$), the result can be simplified to

$$v_\mathbf{i} = c\frac{N-L}{N+L}. \tag{3}$$

The electron propagation (group) velocity corresponds to the derivative of the dispersion relation shown in Fig. 1(a). The energy and momentum are conserved for multiphoton processes, in which $N > L$ and $L > 0$. Because ΔE and Δp_x are small, the derivative can be directly obtained by dividing the energy change $\Delta E \propto (N-L)$ by the momentum change $\Delta p_x \propto (N+L)$. The result of Eq. (3) is visualized using the diagrams in the insets of Fig. 1(a) for three- and four-photon scattering processes.

The initial electron velocity v_i fulfilling the conservation laws can be further adjusted by the experimental geometry, similar to the nonparallel two-photon case [22]. For the electron beam propagating along the x axis interacting with two light waves at a single frequency ω with wave vectors $\boldsymbol{k_1} = (k\cos\alpha, k\sin\alpha, 0)$ and $\boldsymbol{k_2} = (k\cos\beta, k\sin\beta, 0)$ [Fig. 1(c)], the momentum conservation changes to

$$\Delta p_y = \frac{N\hbar\omega}{c}\sin\alpha - \frac{L\hbar\omega}{c}\sin\beta = 0, \tag{4}$$

$$\Delta p_x = \gamma_\mathbf{f} m_0 v_\mathbf{f} - \gamma_\mathbf{i} m_0 v_\mathbf{i} = \frac{N\hbar\omega}{c}\cos\alpha - \frac{L\hbar\omega}{c}\cos\beta. \tag{5}$$

For a given set of initial conditions (v_i, N, L), the solution of Eqs. (1), (4), and (5) defines the angles α and β, for which only the longitudinal component p_x of the electron momentum changes:

$$\cos\beta = \frac{N^2 - L^2 - A^2}{2AL}, \tag{6}$$

$$\sin\alpha = \frac{L}{N}\sqrt{1 - \left(\frac{N^2 - L^2 - A^2}{2LA}\right)^2}, \tag{7}$$

$$A = \frac{m_0c^2}{\hbar\omega}\left\{\sqrt{\left[\frac{(N-L)\hbar\omega}{m_0c^2} + \gamma_\mathbf{i}\right]^2 - 1} - \sqrt{\gamma_\mathbf{i}^2 - 1}\right\} \doteq \frac{(N-L)c}{v_\mathbf{i}}. \tag{8}$$

The detailed derivation of Eqs. (3), (6), (7), and (8) is shown in Appendix A.

The minimum initial electron velocity for the particular set of N and L is given by Eq. (3) and corresponds to $\alpha = 0$ and $\beta = \pi$. Further generalization of the scheme can be performed using different frequencies of the two light fields used to generate the scattering potential or by using more than two light waves interacting with the electron. For each case, the relativistic conservation laws can be used to obtain the necessary angles and frequencies of all beams.

Up to now we discussed the nonlinear scattering processes only from the point of view of energy and momentum conservation. In the following we derive the classical scattering potential for the four-photon process in the simplest geometry shown in Fig. 1(b). The initial electron velocity obtained from Eq. (3) is $v_\mathrm{i} = c/2$. As shown in [36], the classical and quantum mechanical derivations of the scattering potential give the same result in the limit of nonrelativistic field amplitude (normalized amplitude $a = eE/(m_0c\omega) \ll 1$, where e is electron charge) and nonrelativistic electron velocity ($v \ll c$). In our analysis we still assume nonrelativistic field amplitudes. However, relatively high electron velocity before the interaction requires relativistic correction of the classical scattering potential. For

this reason we solve the relativistic equation of motion with the Lorenz force in the laboratory frame:

$$\frac{d}{dt}(\gamma m_0 \boldsymbol{v}) = q(\boldsymbol{E} + \boldsymbol{v} \times \boldsymbol{B}). \tag{9}$$

The electric and magnetic fields of the two counterpropagating plane waves are polarized along the z and y axes, respectively, and have different electric amplitudes E_1 and E_2:

$$E_z = E_1 \cos(\omega t - kx) + E_2 \cos(\omega t + kx), \tag{10}$$

$$B_y = -\frac{E_1}{c}\cos(\omega t - kx) + \frac{E_2}{c}\cos(\omega t + kx). \tag{11}$$

The dynamics occurs only in the x-z plane. The initial conditions for electron coordinates are $\dot{z}(0) = 0, z(0) = 0$, and $\dot{x}(0) = v_{\mathbf{i}}, x(0) = x_{\mathbf{i}}$. The equation of motion is solved using perturbation theory. The electron motion is separated to two components $x = x_{\mathbf{s}} + x_{\mathbf{f}}$ (similar for z) [36]. The fast component x_{f} oscillates at frequency ω and its harmonics, whereas the slow component x_{s} represents a motion time averaged over the optical period. This approach can be applied when the amplitude of x_{f} is much smaller than the wavelength $\lambda = 2\pi c/\omega$. In that case, the first-order term of the Taylor expansion of the fields $E(x,t) \approx E(x_{\mathbf{s}},t) + x_{\mathbf{f}}[dE(x_{\mathbf{s}},t)/dx_{\mathbf{s}}]$ (same for B_y) can be used to obtain different perturbation orders of x_{f}. Further, we assume that x_{s} does not change significantly over one period of the two driving waves $T = 2\pi/\omega$. The relativistic correction to the perturbative series of Eq. (9) is obtained from the expansion of the time derivative of the x and z components of electron momentum in the approximation of a small relative change of the electron velocity $\Delta v/v \ll 1$:

$$\frac{d}{dt}(\gamma m_0 \dot{x}) \doteq \left(\gamma_{\mathbf{i}}^3 \frac{v_{\mathbf{i}}^2}{c^2} + \gamma_{\mathbf{i}}\right) m_0 \ddot{x}, \tag{12}$$

$$\frac{d}{dt}(\gamma m_0 \dot{z}) \doteq \gamma_{\mathbf{i}} m_0 \ddot{z}. \tag{13}$$

Here all the terms containing Δv ($\dot{x}_{\mathbf{f}}$ and $\dot{z}_{\mathbf{f}}$ and their second powers) are neglected. The two coupled equations of motion in this approximation can be written as

$$\ddot{x} = \frac{q}{\left(\gamma_{\mathbf{i}}^3 \frac{v_{\mathbf{i}}^2}{c^2} + \gamma_{\mathbf{i}}\right) m_0} \left\{ -\dot{z}\left[B_y(x_{\mathbf{s}},t) + x_{\mathbf{f}} \frac{dB_y(x_{\mathbf{s}},t)}{dx_{\mathbf{s}}} \right] \right\}, \tag{14}$$

$$\ddot{z} = \frac{q}{\gamma_{\mathbf{i}} m_0} \left\{ \left[E_z(x_{\mathbf{s}},t) + x_{\mathbf{f}} \frac{dE_z(x_{\mathbf{s}},t)}{dx_{\mathbf{s}}} \right] + \dot{x}\left[B_y(x_{\mathbf{s}},t) + x_{\mathbf{f}} \frac{dB_y(x_{\mathbf{s}},t)}{dx_{\mathbf{s}}} \right] \right\}. \tag{15}$$

Equations (14) and (15) are solved by perturbative expansion in powers of the field (for details see Appendix B). The zeroth-order perturbation terms lead to electron motion along the z axis (polarization of the electric field) as the force in the x direction vanishes due to the initial condition $\dot{z}(0) = 0$. The solution of the first-order perturbation yields terms mixing the driving frequency ω with the frequencies of the two waves in the electron rest frame $(1 - v_{\mathrm{i}}/c)\omega$ and $(1 + v_{\mathrm{i}}/c)\omega$. These come from inserting $x_{\mathbf{s}} = v_{\mathbf{i}} t + x_{\mathbf{i}}$ into Eqs. (10) and (11). The classical stationary ponderomotive force is obtained in the limit $v_{\mathbf{i}} \to 0$. For the initial condition corresponding to the four-photon scattering process ($v_{\mathrm{i}} = c/2$), there is no stationary component of the potential acting on the electrons in the first perturbation order. The stationary terms only appear in the second perturbation order, where we get the solution for acceleration along the x axis:

$$\ddot{x} = \frac{q^4 E_1^3 E_2}{m_0^4 c^3 \omega^3 \left(\frac{\gamma_{\mathbf{i}}^3}{4} + \gamma_{\mathbf{i}}\right) \gamma_{\mathbf{i}}^3} \sin(4k x_{\mathbf{i}}). \tag{16}$$

The resulting stationary force is a periodic function of the initial electron position x_{i} with the spatial period of $\lambda/4$. The energy and longitudinal momentum modulation thus occur at frequency 2ω in agreement with the semiclassical picture, where the expected frequency for the four-photon process is given by $3\omega - \omega$. The strength of the interaction depends on the fields of the two waves as $\propto E_1^3 E_2$ corresponding to a process in which three photons are absorbed from the first wave while one photon is emitted to the second wave. A similar analysis can be done for the three-photon process with the initial electron velocity $v_{\mathrm{i}} = c/3$. All the third-order stationary terms $\propto E_1^2 E_2$ vanish in this case because the structure of Eqs. (14) and (15) leads to terms $\ddot{x}$ even in powers of $E_{1,2}$ and $\ddot{z}$ odd in powers of $E_{1,2}$. The only nonvanishing term is $\propto E_1^4 E_2^2 \cos(6k x_{\mathbf{i}})$ coming from the third-order perturbation. This is in agreement with the stationary force in the case of the three-photon process derived in [36], which has two components, $\propto \dot{z} E_1^2 E_2$ and $\propto E_1^4 E_2^2$. The first term vanishes in our case because $z(0) = 0$.

III. RESULTS AND DISCUSSION

The velocity modulation amplitudes for different nonlinear scattering orders are obtained from a numerical solution of the relativistic equation of motion [Eq. (9)] using the fifth-order Runge-Kutta algorithm. In the simulations, the field of each wave is multiplied by a Gaussian temporal envelope $f_{1,2}(x,t) = \exp[-2\ln 2(t \mp x/c)^2/\tau^2]$. The resulting maximum velocity modulation $\Delta v_{\max}/c$ is plotted in Fig. 2(a) as a function of the initial electron velocity v_{i}. The simulation parameters are $\lambda = 800\,\mathrm{nm}$, $\tau = 200\,\mathrm{fs}$, $E_1 = E_2 = 2 \times 10^{11}\,\mathrm{V/m}$ (normalized field amplitude $a = 0.05$, $I = 5.3 \times 10^{15}\,\mathrm{W/cm^2}$, black curve), and $E_1 = E_2 = 5 \times 10^{11}\,\mathrm{V/m}$ ($a = 0.12$, $I = 3.3 \times 10^{16}\,\mathrm{W/cm^2}$, red curve). The resulting peaks correspond to the initial electron velocities obtained using Eq. (3) for different numbers of absorbed and emitted photons N and L. With increasing field amplitudes, higher-order nonlinear processes become accessible. The saturation of the central peak of the red curve is caused by a significant change of the electrons' velocity already during the interaction leading to a more complicated electron dynamics (phase slippage between the electron and the stationary potential, electron channeling, etc.).

The dependence of the amplitude of the electron velocity modulation after the inelastic scattering on the amplitudes E_1 and E_2 was studied for three- [$2\omega - \omega$, Fig. 2(b)], four- [$3\omega - \omega$, Fig. 2(c)], and six-photon [$5\omega - \omega$, Fig. 2(d)] processes. Numerical results correspond well to the analytical perturbative solution of the equation of motion.

Because of the strong dependence of the longitudinal force on the initial electron velocity v_{i}, the proposed nonlinear

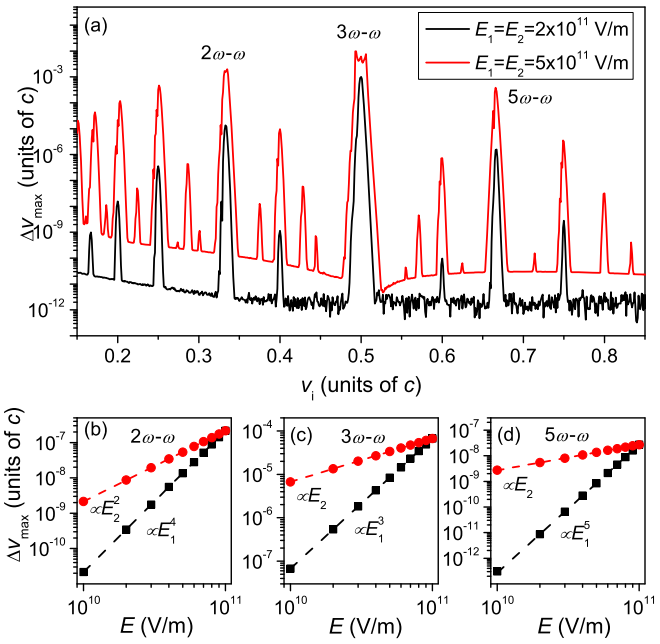

FIG. 2. (a) Amplitude of the velocity modulation $\Delta v_{\max}$ after the interaction of electrons with the optical standing wave obtained from the numerical solution of Eq. (9) as a function of the initial electron velocity v_{i}. Calculations were performed with field amplitudes $E_1 = E_2 = 2 \times 10^{11}$ V/m (black curve) and $E_1 = E_2 = 5 \times 10^{11}$ V/m (red curve). Different nonlinear orders are labeled for three-photon ($2\omega-\omega$), four-photon ($3\omega-\omega$), and six-photon ($5\omega-\omega$) processes. (b–d) Dependence of the final electron velocity modulation on the field amplitudes E_1 ($E_2 = 1 \times 10^{11}$ V/m) and E_2 ($E_1 = 1 \times 10^{11}$ V/m) of the two counterpropagating waves obtained from numerical solution of Eq. (4) for three-, four-, and six-photon processes.

scattering scheme is not well suited for electron acceleration. Furthermore, the scattering efficiency at relativistic electron energies decreases rapidly with increasing γ. For these reasons, the most promising applications are quantum manipulation with free electrons accelerated to moderate energies and attosecond electron compression for ultrafast diffraction and microscopy experiments. In the latter, the high-frequency time-correlated energy modulation obtained during the interaction leads to ballistic compression due to dispersive propagation of the electrons in vacuum [20–23,25,29,34]. A small relative change of the electron's velocity $\Delta v/v_{\mathbf{i}} \ll 1$ during the interaction allows us to describe the scattering process in the impulse approximation. For the four-photon process, the change of the electron velocity as a function of the initial position calculated from Eq. (16) can be written as

$$\Delta v(x_{\mathbf{i}}) = \int_{-\infty}^{\infty} f_1^3(x_{\mathbf{s}},t) f_2(x_{\mathbf{s}},t) \ddot{x} dt = \sqrt{\frac{\pi}{6\ln 2}} \tau \frac{q^4 E_1^3 E_2}{m_0^4 c^3 \omega^3 \left(\frac{\gamma_{\mathbf{i}}^3}{4} + \gamma_{\mathbf{i}}\right) \gamma_{\mathbf{i}}^3} \sin(4k x_{\mathbf{i}}). \quad (17)$$

The result of Eq. (17) is compared with numerical simulations in Fig. 3(a) for the set of electrons with uniform distribution of initial positions $x_i \in \{-\lambda/2, \lambda/2\}$. The introduced energy modulation with amplitude of $\Delta E_{\max} \approx 7$ eV leads to a temporal focus after a propagation distance of $x \approx 1$ mm. The minimum duration of individual electron pulses from the pulse train limited by the Heisenberg uncertainty principle is in this case $\tau_{\mathrm{e,min}} \approx 100$ as [37].

So far, the laser pulses are still treated as plane waves. However, for the experimental observation of the higher-order nonlinear scattering processes, the effects related to the finite size of the laser beams need to be taken into account. To reach the required field amplitude of $E \sim 10^{11}$ V/m with pulse energies of $W < 1$ mJ, the laser beams have to be focused to a small transverse size $w \leqslant 10\,\mu$m. The electrons thus experience a nonstationary ponderomotive force depending on the intensity gradient in the laser focus. The ponderomotive kick to the electrons coming from the rising and the falling edges of the light intensity distribution do not cancel out for short pulses due to the temporal dependence of the light intensity. For small focal sizes ($w < 10\lambda$), the nonlinear scattering contribution to the final electron velocity modulation is combined with the slow ponderomotive modulation due to the intensity gradient in the two laser foci. This is shown in Fig. 3(b), where the interaction of the electrons with the standing wave formed by two Gaussian beams focused to $1/e$ transverse radii of $w_0 = 5\,\mu$m is numerically simulated. The ponderomotive force manifests itself in the slope of the center of the final electron velocity modulation [dashed curve in Fig. 3(b)]. Because of the small focal size of the laser beams leading to a large divergence angle, paraxial approximation is not sufficient for description of the fields in the focal region. Instead, the fields are calculated using the angular spectrum representation of plane waves [38]. The full solution is expanded in powers of $\varepsilon = 1/(kw_0)$ and the first-order correction is used.

The classical scattering theory provides a good approximation for calculating the electron spectra after the interaction for a large energy modulation $\Delta E_{\max} \gg \hbar\omega$. If this condition is not met, the interaction has to be described using quantum theory. As shown in [37], the evolution of the quantum state of the electrons after scattering does not depend on the physical origin of the sinusoidal energy modulation. The Schrödinger equation with the scattering potential obtained from Eq. (16) can be solved using the Crank-Nicolson algorithm in the electron's rest frame. The final energy modulation will contain peaks spaced by $(N-L)\hbar\omega$ from the peak at the initial energy. The short period of the energy modulation allows us to study coherent processes (such as reported in [25,27,29]) using electron beams with a lower degree of longitudinal coherence.

There are several benefits of the proposed scheme compared to other techniques allowing ultrafast control of energy and longitudinal momentum of freely propagating electrons. The techniques based on optical near fields [24–27,29–33] or light field discontinuity at thin dielectric or metallic films [28,34,35] both require a nanostructure being illuminated by a pulsed laser beam. The interaction strength is limited due to the laser damage threshold of the nanostructure. This is not the case in vacuum schemes ([20–23], this paper), where the scattering rate is only limited by the available laser power and ultimately by relativistic effects. The scattering rate of the electrons interacting with optical near fields decays with the distance from the surface on subwavelength scales, virtually limiting the interaction to strongly focused electron beams. Moreover, the longitudinal momentum modulation of the

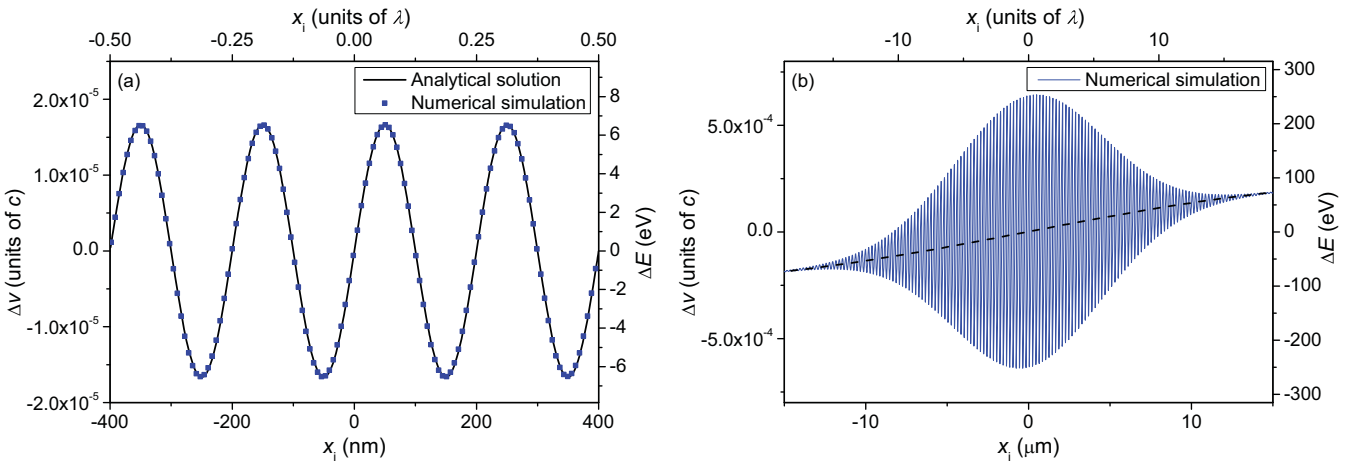

FIG. 3. (a) Electron velocity modulation Δv after the four-photon inelastic scattering. Analytical results obtained from Eq. (17) (curve) are compared to the numerical solution of Eq. (9) (points). Simulation parameters: $\lambda = 800\,\mathrm{nm}$, $\tau = 50\,\mathrm{fs}$, $E_1 = E_2 = 1 \times 10^{11}\,\mathrm{V/m}$, plane wave. (b) Numerical simulation including the finite size of the laser beams. Parameters: $\lambda = 800\,\mathrm{nm}$, $\tau = 50\,\mathrm{fs}$, $E_1 = E_2 = 2.5 \times 10^{11}\,\mathrm{V/m}$, $w_0 = 5\,\mu\mathrm{m}$ leading to the individual pulse energy of $W = 173\,\mu\mathrm{J}$. The dashed curve indicates the shift of the center of the energy modulation due to ponderomotive interaction.

electrons after the near-field interaction is accompanied by the transverse momentum modulation phase shifted by $\pi/2$. The transverse momentum kick can be fully avoided when using thin films, but only for experimental configuration producing tilted attosecond electron pulses [35]. These factors limit the potential applications of both of these techniques.

In contrast, the nonlinear inelastic scattering at an optical standing wave proposed in this paper offers purely longitudinal momentum transfer homogeneous over the transverse profile of the electron beam leading to a formation of a train of nontilted attosecond electron pulses. The maximum transverse size of the electron beam is limited by the transverse dimensions of the laser beams generating the standing wave and the ponderomotive effects due to the spatial distribution of light intensity. The experimental setup using an optical standing wave is less complex than for the ponderomotive electron scattering at an optical traveling wave, where two laser pulses at different frequencies have to be used [20–23].

IV. CONCLUSIONS

In summary, we propose and theoretically investigate a nonlinear inelastic interaction between freely propagating electrons and an optical standing wave. The perturbative analytical solution of the classical relativistic equation of motion leads to a stationary potential in the electron's rest frame. After the interaction, the electron energy is modulated at a harmonic frequency of the driving field. The effect can be observed with subrelativistic field amplitudes achievable with currently available femtosecond lasers, allowing its implementation for ultrafast coherent control of electron beams. Further, as experimentally shown for atoms [2,7] and molecules [39,40], the ponderomotive interaction between an optical standing wave and propagating particles can be enhanced by the presence of electronic resonances or by the molecular polarizability. Similar enhancement can be expected as well for the proposed nonlinear inelastic scattering of atoms and molecules and may enable manipulation with the kinetic energy of neutral particles on subfemtosecond timescales by this technique.

ACKNOWLEDGMENTS

The author would like to thank Prof. P. Hommelhoff for careful reading of the manuscript and for helpful comments. The research was supported by the Gordon and Betty Moore Foundation through Grant No. GBMF4744 "Accelerator on a Chip International Program—ACHIP" and by Charles University (Center of Nano- and Bio-photonics, UNCE/SCI/010).

APPENDIX A: ENERGY AND MOMENTUM CONSERVATION

In this section we show the derivation of Eqs. (3)–(8) from the semiclassical energy and momentum conservation laws. To solve Eqs. (1) and (2) for the case $\alpha = 0$ and $\beta = \pi$, we first express the velocity $v_{\mathrm{i,f}}$ as a function of the Lorentz factor $\gamma_{\mathrm{i,f}}$ as $v_{\mathbf{i,f}} = c\sqrt{1 - \gamma_{\mathbf{i,f}}^{-2}}$. From Eq. (1) we get

$$\gamma_{\mathbf{f}} = \frac{(N - L)\hbar\omega}{m_0 c^2} + \gamma_{\mathbf{i}}. \tag{A1}$$

Inserting these two relations into Eq. (2) leads to Eq. (3):

$$\begin{aligned}\frac{(N+L)\hbar\omega}{c} &= m_0 c\left\{\sqrt{\left[\frac{(N-L)\hbar\omega}{m_0c^2}+\gamma_{\mathbf{i}}\right]^2-1}-\sqrt{\gamma_{\mathbf{i}}^2-1}\right\}\\ &\doteq m_0 c\left[\sqrt{\frac{2(N-L)\hbar\omega\gamma_{\mathbf{i}}}{m_0c^2}+\gamma_{\mathbf{i}}^2-1}-\sqrt{\gamma_{\mathbf{i}}^2-1}\right]=m_0c\sqrt{\gamma_{\mathbf{i}}^2-1}\left[\sqrt{\frac{2(N-L)\hbar\omega\gamma_{\mathbf{i}}}{m_0c^2\left(\gamma_{\mathbf{i}}^2-1\right)}+1}-1\right]\\ &\doteq m_0c\sqrt{\gamma_{\mathbf{i}}^2-1}\frac{(N-L)\hbar\omega\gamma_{\mathbf{i}}}{m_0c^2\left(\gamma_{\mathbf{i}}^2-1\right)}=\frac{(N-L)\hbar\omega\gamma_{\mathbf{i}}}{c\sqrt{\gamma_{\mathbf{i}}^2-1}}=\frac{(N-L)\hbar\omega}{v_{\mathbf{i}}}.\end{aligned}\tag{A2}$$

In Eq. (A2) we assume that $\hbar\omega/(m_0c^2)\ll(\gamma_i^2-1)$. This assumption allows us to use the first-order terms of the Taylor expansion in $\frac{2(N-L)\hbar\omega\gamma_{\mathbf{i}}}{m_0c^2(\gamma_{\mathbf{i}}^2-1)}$ [both $(N-L)$ and $\gamma_{\mathbf{i}}$ are of the order of unity]. For a general choice of angles α and β, the energy and momentum conservation is expressed by Eqs. (4) and (5), from where we obtain

$$\sin\alpha=\frac{L}{N}\sin\beta,\tag{A3}$$

$$N\sqrt{1-\left(\frac{L}{N}\sin\beta\right)^2}-L\cos\beta=\frac{m_0c^2}{\hbar\omega}\left\{\sqrt{\left[\frac{(N-L)\hbar\omega}{m_0c^2}+\gamma_{\mathbf{i}}\right]^2-1}-\sqrt{\gamma_{\mathbf{i}}^2-1}\right\}\doteq\frac{(N-L)c}{v_{\mathbf{i}}}=A,\tag{A4}$$

$$N\sqrt{1-\left(\frac{L}{N}\sin\beta\right)^2}=A+L\cos\beta,\tag{A5}$$

$$N^2\left[1-\left(\frac{L}{N}\sin\beta\right)^2\right]=N^2-L^2+L^2\cos^2\beta=A^2+AL\cos\beta+L^2\cos^2\beta.\tag{A6}$$

Equation (A6) directly leads to Eq. (6). Equation (7) is obtained from Eqs. (A3) and (A6).

APPENDIX B: STATIONARY FORCE COMPONENT FOR FOUR-PHOTON SCATTERING PROCESS

The stationary longitudinal force for the four-photon process given by Eq. (16) is derived from Eqs. (14) and (15) using the conditions for the initial electron velocity obtained from Eq. (3). The slow component of the electron motion $x_{\mathbf{s}}=ct/2+x_{\mathbf{i}}$ is inserted into the formulas defining the fields (transformation of the fields to the electron's rest frame). Starting from the zeroth-order perturbation and using Eqs. (10) and (11), which define the electric and magnetic fields of the two counterpropagating laser beams, we get

$$\ddot{x}^{(0)}=0,\tag{B1}$$

$$\ddot{z}^{(0)}=\frac{q}{\gamma_{\mathbf{i}}m_0}\left[E_z(x_{\mathbf{s}},t)+\dot{x}_{\mathbf{s}}B_y(x_{\mathbf{s}},t)\right]=\frac{q}{\gamma_{\mathbf{i}}m_0}\left\{\frac{E_1}{2}\cos\left(\frac{\omega t}{2}-kx_{\mathbf{i}}\right)+\frac{3E_2}{2}\cos\left(\frac{3\omega t}{2}+kx_{\mathbf{i}}\right)\right\}.\tag{B2}$$

By time integration of Eq. (B2) we obtain the z component of the electron velocity:

$$\dot{z}^{(0)}=\frac{q}{\gamma_{\mathbf{i}}m_0\omega}\left[E_1\sin\left(\frac{\omega t}{2}-kx_{\mathbf{i}}\right)+E_2\sin\left(\frac{3\omega t}{2}+kx_{\mathbf{i}}\right)\right].\tag{B3}$$

The first-order perturbation theory gives

$$\begin{aligned}\ddot{x}^{(1)} &= -\frac{q}{\left(\frac{\gamma_{\mathbf{i}}^3}{4}+\gamma_{\mathbf{i}}\right)m_0}\dot{z}^{(0)}B_y(x_{\mathbf{s}},t)=-\frac{q^2}{\gamma_{\mathbf{i}}\left(\frac{\gamma_{\mathbf{i}}^3}{4}+\gamma_{\mathbf{i}}\right)m_0^2\omega}\left[E_1\sin\left(\tfrac{\omega t}{2}-kx_{\mathbf{i}}\right)+E_2\sin\left(\tfrac{3\omega t}{2}+kx_{\mathbf{i}}\right)\right]\\ &\times\left[-\tfrac{E_1}{c}\cos\left(\tfrac{\omega t}{2}-kx_{\mathbf{i}}\right)+\tfrac{E_2}{c}\cos\left(\tfrac{3\omega t}{2}+kx_{\mathbf{i}}\right)\right]=\frac{q^2}{2\gamma_{\mathbf{i}}\left(\frac{\gamma_{\mathbf{i}}^3}{4}+\gamma_{\mathbf{i}}\right)m_0^2\omega c}\left\{E_1^2\sin(\omega t-2kx_{\mathbf{i}})\right.\\ &\left.+E_1E_2[2\sin(\omega t+2kx_{\mathbf{i}})]-E_2^2\sin(3\omega t+2kx_{\mathbf{i}})\right\},\end{aligned}\tag{B4}$$

$$\dot{x}^{(1)}=\frac{q^2}{2\gamma_{\mathbf{i}}\left(\frac{\gamma_{\mathbf{i}}^3}{4}+\gamma_{\mathbf{i}}\right)m_0^2\omega^2c}\left\{-E_1^2\cos(\omega t-2kx_{\mathbf{i}})-E_1E_2[2\cos(\omega t+2kx_{\mathbf{i}})]+\frac{E_2^2}{3}\cos(3\omega t+2kx_{\mathbf{i}})\right\},\tag{B5}$$

$$x^{(1)}=\frac{q^2}{2\gamma_{\mathbf{i}}\left(\frac{\gamma_{\mathbf{i}}^3}{4}+\gamma_{\mathbf{i}}\right)m_0^2\omega^3c}\left\{-E_1^2\sin(\omega t-2kx_{\mathbf{i}})-E_1E_2[2\sin(\omega t+2kx_{\mathbf{i}})]+\frac{E_2^2}{9}\sin(3\omega t+2kx_{\mathbf{i}})\right\}.\tag{B6}$$

Using the results of Eqs. (B5) and (B6) we can continue to the first-order perturbation in coordinate z. We first write Eq. (15) for $\ddot{z}^{(1)}$:

$$\begin{aligned}
\ddot{z}^{(1)} &= \frac{q}{\gamma_{\mathbf{i}} m_0}\left\{\left[E_z(x_{\mathbf{s}},t)+x_{\mathbf{f}}^{(1)}\frac{dE_z(x_{\mathbf{s}},t)}{dx_{\mathbf{s}}}\right]+\left(\dot{x}_{\mathbf{s}}+\dot{x}_{\mathbf{f}}^{(1)}\right)\left[B_y(x_{\mathbf{s}},t)+x_{\mathbf{f}}^{(1)}\frac{dB_y(x_{\mathbf{s}},t)}{dx_{\mathbf{s}}}\right]\right\}\\
&= \frac{q}{\gamma_{\mathbf{i}} m_0}\left\{\left[E_z(x_{\mathbf{s}},t)+x_{\mathbf{f}}^{(1)}\frac{dE_z(x_{\mathbf{s}},t)}{dx_{\mathbf{s}}}\right]+\dot{x}_{\mathbf{s}}B_y(x_{\mathbf{s}},t)+\dot{x}_{\mathbf{s}}x_{\mathbf{f}}^{(1)}\frac{dB_y(x_{\mathbf{s}},t)}{dx_{\mathbf{s}}}+\dot{x}_{\mathbf{f}}^{(1)}B_y(x_{\mathbf{s}},t)+O(E^5)\right\}\\
&\doteq \ddot{z}^{(0)}+\frac{q^3}{2\gamma_{\mathbf{i}}^2\left(\frac{\gamma_{\mathbf{i}}^3}{4}+\gamma_{\mathbf{i}}\right)m_0^3\omega^2c^2}\left\{-E_1^2\sin(\omega t-2kx_{\mathbf{i}})-E_1E_2[2\sin(\omega t+2kx_{\mathbf{i}})]+\frac{E_2^2}{9}\sin(3\omega t+2kx_{\mathbf{i}})\right\}\\
&\quad\times\left[E_1\sin\left(\frac{\omega t}{2}-kx_{\mathbf{i}}\right)-E_2\sin\left(\frac{3\omega t}{2}+kx_{\mathbf{i}}\right)\right]\\
&\quad+\frac{1}{2}\frac{q^3}{2\gamma_{\mathbf{i}}^2\left(\frac{\gamma_{\mathbf{i}}^3}{4}+\gamma_{\mathbf{i}}\right)m_0^3\omega^2c^2}\left\{-E_1^2\sin(\omega t-2kx_{\mathbf{i}})-E_1E_2[2\sin(\omega t+2kx_{\mathbf{i}})]+\frac{E_2^2}{9}\sin(3\omega t+2kx_{\mathbf{i}})\right\}\\
&\quad\times\left[-E_1\sin\left(\frac{\omega t}{2}-kx_{\mathbf{i}}\right)-E_2\sin\left(\frac{3\omega t}{2}+kx_{\mathbf{i}}\right)\right]\\
&\quad+\frac{q^3}{2\gamma_{\mathbf{i}}^2\left(\frac{\gamma_{\mathbf{i}}^3}{4}+\gamma_{\mathbf{i}}\right)m_0^3\omega^2c^2}\left\{-E_1^2\cos(\omega t-2kx_{\mathbf{i}})-E_1E_2[2\cos(\omega t+2kx_{\mathbf{i}})]+\frac{E_2^2}{3}\cos(3\omega t+2kx_{\mathbf{i}})\right\}\\
&\quad\times\left[-E_1\cos\left(\frac{\omega t}{2}-kx_{\mathbf{i}}\right)+E_2\cos\left(\frac{3\omega t}{2}+kx_{\mathbf{i}}\right)\right].
\end{aligned}\tag{B7}$$

Here we neglected the term $\dot{x}_{\mathbf{f}}^{(1)}x_{\mathbf{f}}^{(1)}\frac{dB_y(x_{\mathbf{s}},t)}{dx_{\mathbf{s}}}$, which depends on E^5. Further, we investigate which terms can contribute to the stationary force component $\ddot{x}^{(2)}$ and neglect all other terms. Multiplication of trigonometric functions in Eq. (B7) leads to terms with phases given by $a\pm b$, where a and b are the initial phases. Because in the next perturbation order, $\dot{z}^{(1)}$ is multiplied by the magnetic field $B_y=[-\frac{E_1}{c}\cos(\frac{\omega t}{2}-kx_{\mathbf{i}})+\frac{E_2}{c}\cos(\frac{3\omega t}{2}+kx_{\mathbf{i}})]$, a stationary component in the second-order perturbation is possible only for terms containing $\frac{\omega t}{2}+nkx_0$ or $s\frac{3\omega t}{2}+mkx_0$, where $n\neq -1, n\in Z$ (Z is an integer number) and $m\neq 1, n\in Z$. The terms with $n=-1$ and $m=1$ will cancel out in $\ddot{x}^{(2)}$, because $\sin(a-b)=\sin(0)=0$ and $\sin(a+b)$ will contain an oscillatory part dependent on ωt. All terms containing $l\omega t$, where $l\in Z$, will cancel out after time averaging over the time period of the field $T=\frac{2\pi}{\omega}$. When we write only the terms, which lead to nonzero stationary components of $\ddot{x}^{(2)}$, we get

$$\begin{aligned}
\ddot{z}^{(1)} &= \ddot{z}^{(0)}+\frac{q^3}{4\gamma_{\mathbf{i}}^2\left(\frac{\gamma_{\mathbf{i}}^3}{4}+\gamma_{\mathbf{i}}\right)m_0^3\omega^2c^2}\left[E_1^3\cos\left(\frac{3\omega t}{2}-3kx_{\mathbf{i}}\right)+E_1^2E_2\cos\left(\frac{\omega t}{2}+3kx_{\mathbf{i}}\right)\right.\\
&\quad-2E_1^2E_2\cos\left(\frac{\omega t}{2}+3kx_{\mathbf{i}}\right)-\frac{1}{2}E_1^3\cos\left(\frac{3\omega t}{2}-3kx_{\mathbf{i}}\right)+\frac{1}{2}E_1^2E_2\cos\left(\frac{\omega t}{2}+3kx_{\mathbf{i}}\right)+E_1^2E_2\cos\left(\frac{\omega t}{2}+3kx_{\mathbf{i}}\right)\\
&\quad\left.+E_1^3\cos\left(\frac{3\omega t}{2}-3kx_{\mathbf{i}}\right)-E_1^2E_2\cos\left(\frac{\omega t}{2}+3kx_{\mathbf{i}}\right)+2E_1^2E_2\cos\left(\frac{\omega t}{2}+3kx_{\mathbf{i}}\right)\right]\\
&= \ddot{z}^{(0)}+\frac{q^3}{4\gamma_{\mathbf{i}}^2\left(\frac{\gamma_{\mathbf{i}}^3}{4}+\gamma_{\mathbf{i}}\right)m_0^3\omega^2c^2}\left[\frac{3}{2}E_1^3\cos\left(\frac{3\omega t}{2}-3kx_{\mathbf{i}}\right)+\frac{3}{2}E_1^2E_2\cos\left(\frac{\omega t}{2}+3kx_{\mathbf{i}}\right)\right],
\end{aligned}\tag{B8}$$

$$\begin{aligned}
\dot{z}^{(1)} &= \dot{z}^{(0)}+\frac{q^3}{4\gamma_{\mathbf{i}}^2\left(\frac{\gamma_{\mathbf{i}}^3}{4}+\gamma_{\mathbf{i}}\right)m_0^3\omega^3c^2}\left[E_1^3\sin\left(\frac{3\omega t}{2}-3kx_{\mathbf{i}}\right)+3E_1^2E_2\sin\left(\frac{\omega t}{2}+3kx_{\mathbf{i}}\right)\right]\\
&= \dot{z}^{(0)}+\dot{z}_{\mathbf{f}}^{(1)}.
\end{aligned}\tag{B9}$$

Now we use the result of Eq. (B9) for the final calculation of $\ddot{x}^{(2)}$:

$$\begin{aligned}
\ddot{x}^{(2)} &= \frac{q}{\gamma_{\mathbf{i}} m_0}\left\{-\dot{z}^{(1)}\left[B_y(x_{\mathbf{s}},t)+x_{\mathbf{f}}^{(1)}\frac{dB_y(x_{\mathbf{s}},t)}{dx_{\mathbf{s}}}\right]\right\}\\
&= \frac{q}{\gamma_{\mathbf{i}} m_0}\left[-\dot{z}^{(0)}B_y(x_{\mathbf{s}},t)-\dot{z}_{\mathbf{f}}^{(1)}B_y(x_{\mathbf{s}},t)-\dot{z}^{(0)}x_{\mathbf{f}}^{(1)}\frac{dB_y(x_{\mathbf{s}},t)}{dx_{\mathbf{s}}}+O(E^6)\right]
\end{aligned}$$

$$
\begin{aligned}
\doteq \ddot{x}^{(1)} &- \frac{q^4}{4\gamma_{\mathbf{i}}^3\left(\frac{\gamma_{\mathbf{i}}^3}{4}+\gamma_{\mathbf{i}}\right)m_0^4\omega^3c^3}\left[E_1^3\sin\left(\frac{3\omega t}{2}-3kx_{\mathbf{i}}\right)+3E_1^2E_2\sin\left(\frac{\omega t}{2}+3kx_{\mathbf{i}}\right)\right] \\
&\times\left[-E_1\cos\left(\frac{\omega t}{2}-kx_{\mathbf{i}}\right)+E_2\cos\left(\frac{3\omega t}{2}+kx_{\mathbf{i}}\right)\right] \\
&- \frac{q^4}{2\gamma_{\mathbf{i}}^3\left(\frac{\gamma_{\mathbf{i}}^3}{4}+\gamma_{\mathbf{i}}\right)m_0^4\omega^3c^3}\left[E_1\sin\left(\frac{\omega t}{2}-kx_{\mathbf{i}}\right)+E_2\sin\left(\frac{3\omega t}{2}+kx_{\mathbf{i}}\right)\right] \\
&\times\left\{-E_1^2\sin\left(\omega t-2kx_{\mathbf{i}}\right)-E_1E_2[2\sin\left(\omega t+2kx_{\mathbf{i}}\right)]+\frac{E_2^2}{9}\sin\left(3\omega t+2kx_{\mathbf{i}}\right)\right\} \\
&\times\left[-E_1\sin\left(\frac{\omega t}{2}-kx_{\mathbf{i}}\right)-E_2\sin\left(\frac{3\omega t}{2}+kx_{\mathbf{i}}\right)\right]. \qquad \text{(B10)}
\end{aligned}
$$

All the terms dependent on powers of $E_{1,2}$ higher than 4 were neglected in Eq. (B10). When we apply the summation rules for trigonometric functions and perform time averaging over the field period, we directly obtain Eq. (16):

$$
\langle\ddot{x}\rangle_T=\frac{\int_0^T\ddot{x}(t)dt}{T}=\frac{q^4E_1^3E_2}{m_0^4c^3\omega^3\left(\frac{\gamma_{\mathbf{i}}^3}{4}+\gamma_{\mathbf{i}}\right)\gamma_{\mathbf{i}}^3}sin(4kx_{\mathbf{i}}). \qquad \text{(B11)}
$$

[1] P. L. Kapitza and P. A. Dirac, Proc. Cambridge Philos. Soc. **29**, 297 (1933).
[2] P. L. Gould, G. A. Ruff, and D. E. Pritchard, Phys. Rev. Lett. **56**, 827 (1986).
[3] D. L. Freimund, K. Aflatooni, and H. Batelaan, Nature (London, UK) **413**, 142 (2001).
[4] D. L. Freimund and H. Batelaan, Phys. Rev. Lett. **89**, 283602 (2002).
[5] P. H. Bucksbaum, M. Bashkansky, and T. J. McIlrath, Phys. Rev. Lett. **58**, 349 (1987).
[6] P. H. Bucksbaum, D. W. Schumacher, and M. Bashkansky, Phys. Rev. Lett. **61**, 1182 (1988).
[7] S. Eilzer, H. Zimmermann, and U. Eichmann, Phys. Rev. Lett. **112**, 113001 (2014).
[8] M. A. Efremov and M. V. Fedorov, J. Exp. Theor. Phys. **89**, 460 (1999).
[9] X. Li, J. Zhang, Z. Xu, P. Fu, D.-S. Guo, and R. R. Freeman, Phys. Rev. Lett. **92**, 233603 (2004).
[10] Y. W. Chan and W. L. Tsui, Phys. Rev. A **20**, 294 (1979).
[11] P. J. Martin, B. G. Oldaker, A. H. Miklich, and D. E. Pritchard, Phys. Rev. Lett. **60**, 515 (1988).
[12] P. W. Smorenburg, J. H. M. Kanters, A. Lassise, G. J. H. Brussaard, L. P. J. Kamp, and O. J. Luiten, Phys. Rev. A **83**, 063810 (2011).
[13] A. E. Kaplan and A. L. Pokrovsky, Phys. Rev. Lett. **95**, 053601 (2005).
[14] S. Ahrens, H. Bauke, C. H. Keitel, and C. Müller, Phys. Rev. A **88**, 012115 (2013).
[15] D. Bauer, P. Mulser, and W. H. Steeb, Phys. Rev. Lett. **75**, 4622 (1995).
[16] S. McGregor, W. C.-W. Huang, B. A. Shadwick, and H. Batelaan, Phys. Rev. A **92**, 023834 (2015).
[17] R. Erhard and H. Bauke, Phys. Rev. A **92**, 042123 (2015).
[18] S. Ahrens, H. Bauke, C. H. Keitel, and C. Müller, Phys. Rev. Lett. **109**, 043601 (2012).
[19] M. M. Dellweg and C. Müller, Phys. Rev. A **95**, 042124 (2017).
[20] P. Baum and A. H. Zewail, Proc. Natl Acad. Sci. USA **104**, 18409 (2007).
[21] S. A. Hilbert, C. Uiterwaal, B. Barwick, H. Batelaan, and A. H. Zewail, Proc. Natl. Acad. Sci. USA **106**, 10558 (2009).
[22] M. Kozák, T. Eckstein, N. Schönenberger, and P. Hommelhoff, Nat. Phys. **14**, 121 (2018).
[23] M. Kozák, N. Schönenberger, and P. Hommelhoff, Phys. Rev. Lett. **120**, 103203 (2018).
[24] B. Barwick, D. J. Flannigan, and A. H. Zewail, Nature (London, UK) **462**, 902 (2009).
[25] A. Feist, K. E. Echternkamp, J. Schauss, S. V. Yalunin, S. Schäfer, and C. Ropers, Nature (London, UK) **521**, 200 (2015).
[26] L. Piazza, T. T. A. Lummen, E. Quiñonez, Y. Murooka, B. W. Reed, B. Barwick, and F. Carbone, Nat. Commun. **6**, 6407 (2015).
[27] K. E. Echternkamp, A. Feist, S. Schäfer, and C. Ropers, Nat. Phys. **12**, 1000 (2016).
[28] F. O. Kirchner, A. Gliserin, F. Krausz, and P. Baum, Nat. Photonics **8**, 52 (2014).
[29] K. E. Priebe, C. Rathje, S. V. Yalunin, T. Hohage, A. Feist, S. Schäfer, and C. Ropers, Nat. Photonics **11**, 793 (2017).
[30] E. A. Peralta, K. Soong, R. J. England, E. R. Colby, Z. Wu, B. Montazeri, C. McGuinness, J. McNeur, K. J. Leedle, D. Walz, E. B. Sozer, B. Cowan, B. Schwartz, G. Travish, and R. L. Byer, Nature (London, UK) **503**, 91 (2013).
[31] J. Breuer and P. Hommelhoff, Phys. Rev. Lett. **111**, 134803 (2013).

[32] M. Kozák, J. McNeur, K. J. Leedle, H. Deng, N. Schönenberger, A. Ruehl, I. Hartl, J. S. Harris, R. L. Byer, and P. Hommelhoff, Nat. Commun. **8**, 14342 (2017).
[33] M. Kozák, J. McNeur, K. J. Leedle, H. Deng, N. Schönenberger, A. Ruehl, I. Hartl, H. Hoogland, R. Holzwarth, J. S. Harris, R. L. Byer, and P. Hommelhoff, Opt. Lett. **41**, 3435 (2016).
[34] Y. Morimoto and P. Baum, Nat. Phys. **14**, 252 (2018).
[35] Y. Morimoto and P. Baum, Phys. Rev. A **97**, 033815 (2018).
[36] O. Smirnova, D. L. Freimund, H. Batelaan, and M. Ivanov, Phys. Rev. Lett. **92**, 223601 (2004).
[37] P. Baum, J. Appl. Phys. **122**, 223105 (2017).
[38] B. Quesnel and P. Mora, Phys. Rev. E **58**, 3719 (1998).
[39] S. Gerlich, L. Hackermüller, K. Hornberger, A. Stibor, H. Ulbricht, M. Gring, F. Goldfarb, T. Savas, M. Müri, M. Mayor, and M. Arndt, Nat. Phys. **3**, 711 (2007).
[40] O. Nairz, B. Brezger, M. Arndt, and A. Zeilinger, Phys. Rev. Lett. **87**, 160401 (2001).